DOI:
10.1016/j.chemphyslip.2017.06.007

Document Version
Peer reviewed version

Title: The influence of mild acidity on lysyl-phosphatidylglycerol biosynthesis and lipid membrane physico-chemical properties in methicillin-resistant *Staphylococcus aureus*

Authors: Reg P. Rehal, Helene Marbach, Alasdair T.M. Hubbard, Anam A. Sacranie, Federica Sebastiani, Giovanna Fragneto, Richard D. Harvey

PII: S0009-3084(17)30120-2
DOI: http://dx.doi.org/doi:10.1016/j.chemphyslip.2017.06.007
Reference: CPL 4571

To appear in: *Chemistry and Physics of Lipids*

Received date: 9-5-2017
Revised date: 20-6-2017
Accepted date: 20-6-2017

Please cite this article as: Rehal, Reg P., Marbach, Helene, Hubbard, Alasdair T.M., Sacranie, Anam A., Sebastiani, Federica, Fragneto, Giovanna, Harvey, Richard D., The influence of mild acidity on lysyl-phosphatidylglycerol biosynthesis and lipid membrane physico-chemical properties in methicillin-resistant Staphylococcus aureus.Chemistry and Physics of Lipids http://dx.doi.org/10.1016/j.chemphyslip.2017.06.007

The influence of mild acidity on lysyl-phosphatidylglycerol biosynthesis and lipid membrane physico-chemical properties in methicillin-resistant *Staphylococcus aureus*.

Reg P. Rehal[1], Helene Marbach[1,b], Alasdair T. M. Hubbard[1,4], Anam A. Sacranie[1], Federica Sebastiani[3,a], Giovanna Fragneto[3], Richard D. Harvey[1,2]*.

[1]Institute of Pharmaceutical Science, King's College London, London, UK.

[2]Institute of Pharmacy, Martin-Luther-Universität Halle-Wittenberg, Halle (Saale), Germany.

[3]Institut Laue Langevin, 71 avenue des Martyrs, BP 156, 38100 Grenoble, France.

[4]Nuffield Department of Clinical Medicine, University of Oxford, Oxford, United Kingdom

*e-mail: richard.harvey@pharmazie.uni-halle.de

Current affiliations:

[a]CR Competence AB, Lund, Sweden & Department of Physical Chemistry, Lund University, Lund, Sweden.

[b]Functional Microbiology, Institute of Microbiology, Department of Pathobiology, University of Veterinary Medicine Vienna, Veterinärplatz 1, AT-1210 Vienna, Austria.

Graphical Abstract

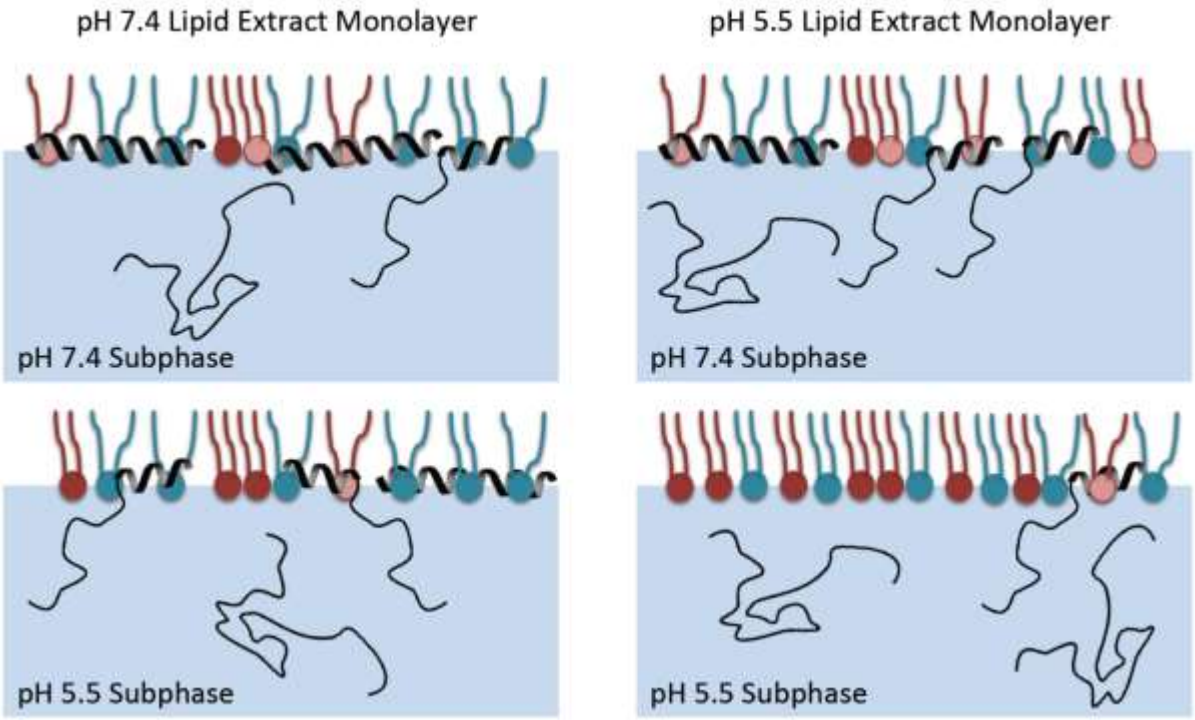

<InlineImage1>

Highlights

- 1. ^{31}P NMR provides a sensitive and non-destructive method for lipidomic analysis of bacterial membranes containing labile aminoacyl phosphatidylglycerols.
- 2. Effective membrane neutralisation in bilayers containing lysyl-phosphatidylglycerol is only achieved under mildly acidic conditions.
- 3. Lipid ion-pairing in bacterial lipid extracts containing fully-ionised lysyl-phosphatidylglycerol elicits modest ordering effects detectable in air/water interface monolayers.
- 4. Increased quantities of fully-ionised lysyl-phosphatidylglycerol in model bacterial membranes significantly reduce binding and partitioning of antimicrobial peptides.

Abstract

The increased biosynthesis of lysyl-phosphatidylglycerol in *Staphylococcus aureus* when cultured under conditions of mild acidity and the resultant increased proportion of this lipid in the plasma membrane of the bacterium, alters the physico-chemical properties of lipid bilayers in a manner which is itself dependent upon environmental pH. Clinically relevant strains of *S. aureus*, both methicillin susceptible and resistant, all exhibited increased lysyl-phosphatidylglycerol biosynthesis in response to mild environmental acidity, albeit to differing degrees, from ~30% to ~55% total phospholipid. Polar lipid extracts from these bacteria were analysed by ^{31}P NMR and reconstituted into vesicles and monolayers, which were characterised by zeta potential measurements and Langmuir isotherms respectively. A combination of increased lysyl-phosphatidylglycerol content and mild environmental acidity were found to synergistically neutralise the charge of the membranes, in one instance altering the zeta potential from –62 mV to +15 mV, and induce closer packing

between the lipids. Challenge of reconstituted *S. aureus* lipid model membranes by the antimicrobial peptide magainin 2 F5W was examined using monolayer subphase injection and neutron diffraction, and revealed that ionisation of the headgroup α–amine of lysyl-phosphatidylglycerol at pH 5.5, which reduced the magnitude of the peptide-lipid interaction by 80%, was more important for resisting peptide partitioning than increased lipid content alone. The significance of these results is discussed in relation to how colonising mildly acidic environments such as human mucosa may be facilitated by increased lysyl-phosphatidylglycerol biosynthesis and the implications of this for further biophysical analysis of the role of this lipid in bacterial membranes.

KeyWords: Lysyl-phosphatidylglycerol; Mild acidity; Monolayers; Neutron diffraction; Antimicrobial resistance

1 Introduction

The mildly acidic conditions encountered at a number of human epithelia constitute part of the intrinsic barrier to bacterial colonisation and infection. The fact that these epithelial surfaces are colonised by a number of different species of commensal bacteria suggests that these organisms have evolved mechanisms for tolerating the localised level of acidity and other intrinsic defences exhibited by their hosts (Hornef et al., 2005). In the case of opportunistic pathogens such as *Staphylococcus aureus*, the ability to survive under the pressure of such epithelial defences may also provide some clues as to their ability to invade soft tissues and establish infections.

The link between resistance to the human antimicrobial peptides (AMP) which form part of the innate immune defences at epithelia and changes in the plasma membrane phospholipid composition of *S. aureus* has long been established *(*Li *et al.*, 2007). Increasing biosynthesis of the cationic lipid lysyl-phosphatidylglycerol (L-PG) via the upregulation of the membrane-integral lysyl transferase MprF, facilitates resistance to cationic AMP *in vitro* via the putative neutralisation of the plasma membrane charge as the proportion of L-PG reaches parity with anionic lipids (mostly phosphatidylglycerol) (Andra *et al*., 2011; Staubitz *et al*., 2004). Mildly acidic environments also increase the biosynthesis of L-PG in *S. aureus*, and may play a more important part in its functional role than has hitherto been considered (Denich *et al*., 2003; Nesbitt and Lennarz, 1968). Since the L-PG headgroup (fig. 1) possesses three ionisable groups with distinct pK_a values (Tocanne *et al*., 1974), the local pH of the lipid will determine whether or not it is likely to form ion-pairs with adjacent anionic lipids to facilitate plasma membrane neutralisation. The pK_a of the L-PG headgroup α-amine has been determined to be ~7.0 making plasma membrane neutralisation more likely in mildly acidic environments (Tocanne *et al*., 1974), which may explain why earlier *in vitro* assessments of the role of L-PG in AMP resistance yielded equivocal results (Khatib *et al*., 2016; Kilelee *et al*., 2010).

Biophysical assessment of the role of L-PG in resistance to cationic antimicrobials has been hampered by the highly labile nature of the lipid under neutral and mildly alkaline conditions (Danner *et al*., 2008), as this means that it is readily hydrolysed when subjected to vesicle manufacturing procedures such as ultrasonication and analysis techniques such as x-ray diffraction. This has led to the synthesis of stable analogues of L-PG (Cox *et al*., 2014; Rehal, 2014) which can be used more effectively in biophysical experiments with long measurement timescales, which aim to elucidate the physical mechanisms of membrane defence facilitated by L-PG in synthetic membranes. In this study, we have attempted to circumvent the problem of L-PG instability by using freshly prepared polar lipid extracts (analysed using ^{31}P-NMR) from different clinically relevant methicillin resistant *S. aureus* (MRSA) strains, in rapid biophysical assays performed to assess the physical effects of L-PG in reconstituted lipid membranes and the putative roles of membrane lipid composition and environmental pH in AMP resistance.

We have examined the effect of both L-PG content and pH on MRSA lipid extracts in membrane mimetic monolayers and bilayers using a combination of Langmuir isotherms and zeta-potential measurements. The degree to which such systems can

resist interaction with the model AMP magainin 2 F5W at pHs mimicking those of the skin (pH ~5.5) and blood compartments of the body (pH 7.4), was determined by adapting the monolayer technique to measure peptide partitioning after subphase injection, and by assessing the depth of peptide penetrating into MRSA lipid bilayers using neutron diffraction. In addition to these physico-chemical studies we also conducted a phenotypic analysis of the effects of mild acidity on L-PG biosynthesis in our MRSA strains, using ^{31}P NMR lipidomics. Our findings show that pH not only influences membrane lipid composition, but it also directly affects membrane charge, rigidity and AMP interaction.

2 Materials and Methods

2.1 Materials

Brain heart infusion (BHI) media was used for all bacterial cultures and was purchased from Oxoid, UK. Concentrated hydrochloric acid (12.4 M, 38.0%), ethanol (99.9%), d-chloroform with 0.03% (v/v) tetra-methyl silane (≥99.8 %D atom), ethylenediaminetetraacetic acid (≥98.0%), tris(hydroxymethyl)aminomethane (>99.0%), glacial acetic acid, sodium sulphate (>99.0%), deuterium oxide (99.9%), sucrose (≥99.5%) and sodium chloride ACS reagent (≥99.0%), were all purchased from Sigma-Aldrich, UK, and used as supplied. Methanol, chloroform and ethanol were purchased from Fisher Scientific, UK, and used as supplied. 1,2-*O*-dipalmitoyl-*sn*-glycero-3-phospho-(1'-*rac*-glycerol) sodium salt (DPPG), 1,2-*O*-dipalmitoyl-*sn*-glycero-3-[phospho-*rac*-(3-lysyl(1-glycerol))] chloride salt (DPL-PG) and 1,1',2,2'-tetramyristoyl cardiolipin ammonium salt (TMCL) were all purchased with >99.0% purity from Avanti Polar Lipids, USA.

2.2 Bacterial Strains

The five *S. aureus* clinical isolates used in this study (Table 1) were kindly provided by the Centre for Clinical Infection and Diagnostics Research (CIDR), at Guy's and St. Thomas' NHS Foundation Trust Hospital in London, UK (GSTT). All these strains were isolated from bacteraemia patients hospitalised between 2001 and 2009. The strains were selected on the basis of CIDR in-house testing and data assessment, which identified their clonal group assignment (multi-locus sequence type and Spa type), together with their methicillin resistance status and vancomycin minimum inhibitory concentrations (MIC).

2.3 Phospholipid extraction and quantification

Each strain of *S. aureus* (Table 1) was pre-cultured in 50 ml BHI broth for 18 hours at 37°C with continuous shaking at 100 rpm. A 1 ml aliquot from each specific pre-culture was then used to inoculate 400 ml of BHI broth with initial pHs of either 7.4, or 5.5 (adjusted with concentrated hydrochloric acid prior to sterilisation). The culture was then incubated in 400 ml BHI for 18 hours at 37°C with constant shaking at 100 rpm. After incubation, the bacterial suspension was centrifuged on a Beckman Coulter J2-21 (Beckman Coulter, UK) at 10 000 rpm for 20 minutes at 4°C and the resulting pellet was washed twice with 50 ml of 150 mM sodium chloride solution adjusted to either pH 5.5 or 7.4 (depending on the initial culture pH), by vortexing the pellet until it was fully resuspended and then centrifuging again at 10 000 rpm for 20 minutes at 4°C.

The polar lipids were extracted using an adapted Bligh and Dyer (Bligh and Dyer, 1959) method in order to preserve the alkali-labile L-PG. Two grams of the washed bacterial pellet were vortexed for 5 minutes with 40 ml of chloroform/methanol solution (2:1 v/v) and 0.26 ml of 2 M HCl to create a single phase. The mixture was then incubated for 90 minutes at 37°C with 100 rpm agitation prior to the addition of 16.6 mL of 150 mM sodium chloride solution (pH 2.0), to create two separate phases. The two-phase system was vortexed for 5 minutes and then centrifuged

using a Beckman Coulter Allegra X-12 (Beckman Coulter, UK) at 3750 rpm for 30 minutes at 20°C. The upper aqueous phase was removed and any insoluble cell debris present at the interface between the phases was discarded. The lower organic layer was then added to 13.2 ml methanol and 16.6 ml of pH 2.0 saline (acidified with concentrated HCl) and centrifuged again at 3750 rpm for 30 minutes at 20°C. The upper aqueous layer was removed and any residual solvents were evaporated under reduced pressure and the resultant lipid film dissolved in a d-chloroform/methanol/sodium chloride (150 mM, pH 2) solution (2:1:0.1 v/v/v). The lipid extraction method was repeated in triplicate with all *S. aureus* strains (Table 1) to obtain the mean relative abundance of the phospholipids in each strain.

^{31}P NMR was performed on the lipid extract samples in addition to DPPG, DPL-PG and TMCL standards at 298.1K and 161.98 MHz, using a Bruker 400 NMR spectrometer (Bruker, Karlsruhe, Germany). The spectra obtained were decoupled against ^{1}H at 400 MHz. All samples were scanned for 3000 cycles at 10 µs pulses. Spectral peaks corresponding to the *S. aureus* phospholipids were then compared to those obtained from the lipid standards and were fitted with a Voigt area function using the program Peakfit Version 4.12 (Systat software, San Jose, USA), to determine relative quantities of the phospholipids present (Systat software 2012). The fitted areas obtained for Cardiolipin were divided by a factor of two to take into account the presence of two phosphate groups in the lipid.

2.4 Pressure-area isotherms of *S. aureus* polar lipid extract monolayers

Solutions of *S. aureus* lipid extracts in chloroform (1 mg/ml) were deposited dropwise onto the surface of a Nima 612D Langmuir trough (NIMA technologies, Coventry, UK) containing an aqueous subphase of 10 mM Tris–acetate (1:1 mol/mol) buffer adjusted to either pH 5.5 or 7.4 with concentrated HCl. The lipid monolayer was equilibrated for 15 min prior to data acquisition to allow all residual chloroform to evaporate and then isotherms were collected through ten cycles at 23°C with a barrier speed of 25 cm^2/min, in triplicate. For each cycle, the maximum surface pressure of the monolayer was limited to 40 mN/m and the minimum surface pressure was set at 0 mN/m. In order to obtain isotherms as plots of surface pressure against molecular area, the average molecular weight of the lipids in each extract (Table 2) was estimated from their proportions as determined by ^{31}P NMR using previously published data reporting *S. aureus* fatty acid quantification (Singh et al., 2008) and the likely counter ions present in the subphase.

The area per molecule for each lipid extract (A_0) was then calculated by extrtapolating the tangent to the isotherm at ~40 mN/m to intercept with the x-axis. The surface compressional modulus (K^s) (Gaines, 1966) for each extract was then calculated using:

$$K^S = -A_0\left(\frac{\delta\Pi}{\delta A}\right) \qquad (1)$$

where, Π is the surface pressure in mN/m.

The compressional modulus is a quantitative measure of the elasticity of a monolayer as a function of molecular area and provides an insight into the phase

transitions present in the isotherm. A K^s value between 50 and 100 mN/m is considered to be characteristic of the liquid expanded (LE) phase, whereas a value between 100 and 250 mN/m is characteristic of the liquid condensed (LC) phase (Dynarowicz-Latka and Hac-Wydro, 2004).

2.5 Zeta potential measurements on *S. aureus* polar lipid extract vesicles

Vesicle dispersions were produced from *S. aureus* lipid extracts by solvating dried lipid films with 10 mM Tris-acetate buffer adjusted to either pH 5.5 or 7.4. Multi-lamellar vesicles (MLVs) of the bacterial lipid extracts were formed by freeze-thaw cycling between -200°C with liquid nitrogen and 50°C in a water bath. The bacterial MLVs were then annealed at 25°C for 60 min prior to measuring their zeta potential.

Zeta potential measurements were carried out on the reconstituted lipid extract vesicles, dispersed in 10 mM Tris–acetate buffer (at both pH 5.5 and 7.4) at 25°C with a Zetasizer Nano ZS (Malvern Instruments Ltd. Worcestershire, UK) using 750 µl folded capillary cells (Malvern Instruments Ltd., UK). The measurement parameters for refractive index and viscosity were set to 1.333 and 0.8872 cP respectively. The samples were measured in triplicate for all lipid extracts from all *S. aureus* strains at both pHs.

2.6 Subphase injection of magainin 2 F5W antimicrobial peptide

Monolayers of *S. aureus* 476 bacterial lipid extracts, harvested from batch cultures grown at either pH 7.4 or pH 5.5, were deposited at the air/liquid interface of a custom-made 110 ml polytetrafluoroethane trough with a surface area of the 86.2 cm^2, in order to achieve a stable surface pressure of ~30 mN/m at 23°C. The aqueous subphase consisted of 10 mM Tris-acetate buffer adjusted to either pH 5.5 or 7.4. The deposited monolayers were allowed to stabilize under constant gentle agitation using a magnetic stirring plate placed beneath the trough, whilst the surface pressure was constantly monitored using a PS4 pressure sensor (Nima Technology, Coventry, U.K.) fitted with a Wilhelmy plate (Whatman 1 Chr). After achieving a stable measurement of the surface pressure for 200 s, 200 µl of magainin 2 F5W at a concentration of 400 µM, dissolved in the appropriate buffer, was injected underneath the monolayer, the surface pressure being continuously recorded until0020no further changes were observed. The final concentration of peptide in the subphase was 3.6 µM, which is above the concentration at which magainin 2 is sufficiently surface active ($\delta\Pi$ > 20

mN/m) to achieve maximal interfacial adsorption in subphases of varying ionic strengths (Bucki *et al*., 2004; Lad *et al*., 2007). Using the estimates for the mean molecular weights of the *S. aureus* 476 lipid extracts reported in Table 2 and their mean molecular areas at 30 mN/m (Figure 3), the average number of lipid molecules deposited at the air/liquid interface was calculated to be ~2 × 10^{16}. The number of magainin 2 F5W molecules injected into the bulk was ~2.4 × 10^{16}, giving a lipid/peptide molar ratio of 1:1.2. All samples were run in triplicate and data was then analysed by plotting the change in surface pressure (δΠ) against time (*t*) after peptide injection and fitting the curves using a Gompertz function (Winsor, 1932), in order to obtain kinetic parameters to compare the rate surface pressure change resulting from the peptide partitioning into each monolayer:

$$\delta\Pi = \delta\Pi_{max} \cdot e^{-e^{-\left(\frac{(t-t_i)}{k}\right)}} \qquad (2)$$

Where δΠ is the change in surface pressure in mN/m, t_i is the time taken in seconds to reach the inflection point of the sigmoidal curve, and *k* is the overall rate constant in s^{-1}.

2.7 Neutron diffraction of *S. aureus* lipid extracts

Orientated multilayers were produced from 10 mg samples of polar lipid extracts from *S. aureus* 476 grown at either pH 5.5 or 7.4, by evenly depositing the lipids onto the polished faces of two separate pre-cleaned 50.8 ± 0.5 mm diameter, 275 ± 20 μm thick silicon wafers (Silicon Materials, Kaufering, Germany) from 1 ml chloroform solutions. Samples of the two lipid extracts containing magainin 2 F5W (at lipid/peptide molar ratios of 50:1) were prepared in the same way, by co-deposition from solution in chloroform. The silicon discs were then stored under a low-pressure atmosphere to ensure that all the chloroform was evaporated. The coated discs were then placed above a saturated Na_2SO_4 bath in a hermetically sealed vessel (to obtain an atmosphere with ~85% relative humidity) and incubated for 24 hours at 50°C. The coated discs were mounted on to a goniometer placed in a sealed temperature-controlled aluminium chamber on the D16 neutron diffractometer beamline at the Institut Laue-Langevin (Grenoble, France) (Sebastiani *et al*., 2012). The humidity and sample contrasts were controlled by using the D16 humidity chamber (Perino-Gallice *et al*., 2002) and varying the H_2O or D_2O content of the internal bath reservoir at different temperatures (21-25°C), whilst the temperature at the sample position was maintained at a constant 25°C.

The samples were examined by neutron diffraction using a beam of 4.74 Å wavelength neutrons with a 1% spread, focused at the sample position by a pyrolitic

graphite monochromator, with a fixed detector distance of 1 m. Diffraction profiles (Intensity vs. 2θ) were compiled for each sample by performing sample angle (θ) scans at various fixed detector positions. Strong reflections were measured for short times (~30 min) whereas weaker ones were measured for ~2-3 hours to improve the signal to noise ratio of the higher orders of diffraction. The diffraction profiles (Intensity vs. Q) for each sample were fitted with an exponential function using Sigmaplot V 12.0 (Systat Software, San Jose, California, USA) to subtract the background scattering. The corrected diffraction peaks were then individually modelled with a Voigt area function to calculate the neutron diffraction peak area ($I(h)$), amplitude (a_0), centre (a_1), width (a_2) and shape (a_3) parameters:

$$I(h) = \frac{a_0.a_3}{\pi\sqrt{\pi.a_2}} \int_{-\infty}^{\infty} \frac{exp(-t^2)}{a_2^2 + \left(\frac{x-a_1}{a_2} - t\right)^2} \cdot dt \qquad (3)$$

Where, h is the order of neutron diffraction.

The mean value of a_1 from each order of diffraction (n) was then used to calculate the lamellar repeat spacing (d-spacing, ψ):

$$\psi = n\lambda/2\sin\theta \qquad (4)$$

To reconstruct the one-dimensional bilayer SLD profile, the absolute bilayer structure factor ($F(h)$) of each order of neutron diffraction were required. $F(h)$ is related to the intensity of the neutron diffraction order, $I(h)$, using (Saxena and Schoenborn, 1977):

$$|F(h)| = \frac{\sqrt{I(h)}}{\sqrt{L_1(h)L_2(h)L_3(h)}} \qquad (5)$$

Where, $L_1(h)$ is the angular velocity term 1/sin 2θ, $L_2(h)$ is a factor correcting for sample mosaicity and $L_3(h)$ is a factor correcting for sample absorption and geometry (Saxena and Schoenborn, 1977).

The correctional factors $L_2(h)$ and $L_3(h)$ were determined by using the D16 instrument Large Array Manipulation Program (LAMP) software (Richard *et al*., 1996), however $L_1(h)$ was determined whilst calculating the structure factors (Leonard *et al*., 2001). Due to the sample being centrosymmetric, the sign of $F(h)$ for each order could have been positive or negative. Therefore to determine the sign of $F(h)$, contrast variation was employed with both H_2O and D_2O contrasts where the linear dependence of $F(h)$ at a given order, h, was determined versus D_2O content (Worcester and Franks, 1976) (see Supporting Information). Following $F(h)$ sign assignment the Patterson map or relative SLD profile of the bilayer in real space perpendicular to the bilayer interface, $p(z)$,was calculated using (Buldt *et al*., 1979; Pebaypeyroula *et al*., 1994):

$$p(z) = \frac{2}{\psi}\sum_{h=1}^{h_{max}} F(h)\cos\left(\frac{2\pi hz}{\psi}\right) \qquad (6)$$

Where, z (the bilayer normal) is the direction perpendicular to the plane of the bilayer.

3 Results

3.1 Polar lipid extract phospholipid quantification

Prior to the analysis of the bacterial lipid extracts, standards of dipalmitoyl lysyl-phosphatidylglycerol (DPL-PG), dipalmitoylphosphatidylglycerol (DPPG) and tetramyristoyl cardiolipin (TMCL) were examined in order to detect their chemical shift values in a ^{31}P NMR spectrum (Figure 2A). The resonance signals of both DPL-PG and TMCL appeared as singlets, which suggested their phosphates adopt a single charge state under the slightly acidic conditions employed. In the case of TMCL which possesses two phosphate groups, under the conditions used for the measurement, the negative charge is shared between the phosphates due to an internal hydrogen bond (Figure 1), therefore both phosphates experience the same magnetic environment giving rise to the single resonance signal in the ^{31}P NMR spectrum (Haines, 2009). Two resonance signals would also be expected for DPL-PG under mildly acidic conditions, due to the existence of ionised and unionised phosphate in the lipid in this environment (L-PG phosphate pK_a ~1-3) (Tocanne *et al*., 1974), however this was not observed. The appearance of one resonance signal for DPL-PG was most likely due to the phosphate always presenting as unionized, as a result of shielding via protonation or by association with either of the protonated amine groups of the lipid headgroup. The only resonance signal for which a split could be detected was DPPG, where a small additional upfield signal was observed (Figure 2A). The presence of an additional resonance signal in the DPPG spectrum suggested the phosphate of DPPG was experiencing two different magnetic environments, possibly due to association with different counter-ions.

The ^{31}P NMR spectra obtained for the natural lipid extracts from all the *S. aureus* strains varied markedly in position and intensity of the PG peaks (Figure 2B). This large variation in PG peak appearance was most likely due to the uncontrolled types of counter-ions present in the lipid extracts, which may have had different charge densities and shielding effects on the PG phosphate. However, these inconsistencies in the appearance of the PG resonance signals posed little problem for the relative lipid quantification of PG, the peaks were easily identified by chemical shift then fitted separately and summed in the final analysis to give an accurate relative quantification of the PG in the lipid extract (Table 2).

Considering the phospholipid content of the five *S. aureus* strains used in this study, only MRSA G33 showed no significant difference in phospholipid composition at pH 5.5 compared to pH 7.4 ($p > 0.05$, Mann–Whitney U test). All of the other *S. aureus* strains tested showed a significant increase in the proportion of L-PG and a concomitant decrease in PG content at pH 5.5 compared to pH 7.4 ($p < 0.05$, Mann–Whitney U test) (Table 2). Interestingly, the growth yield of MRSA G33 gave a final wet weight of ~0.2 g from 400 ml BHI media at pH 5.5, compared to ~0.4 g at pH 7.4. Such a low yield at pH 5.5 suggested the bacteria had low tolerance to the pH 5.5 growth conditions. For all of the other strains, final growth yields of ~0.5 g wet weight were obtained from 400 ml BHI media cultures at both pH 7.4 and 5.5 and displayed L-PG content close to ~50% total phospholipid content at pH 5.5 (Table 2) which is consistent with previous findings (Gould and Lennarz, 1970).

3.2 Pressure-area isotherms of *S. aureus* polar lipid extract monolayers

The pressure-area isotherms obtained from *S. aureus* lipid extracts grown under different culture conditions and measured on subphases at either pH 5.5 or 7.4 (Figure 3) show a high degree of variability in both lift-off pressure and average molecular area at 40 mN/m, whilst retaining similar overall expanded monolayer characteristics. This variability was most likely due to the presence of impurities in the lipid extracts, which would have led to inaccuracies in the calculation of their average molecular weights (Table 2). Therefore, when it comes to comparing physical characteristics between the monolayers, measures which require the calculation of extrapolated areas per molecule (such as the surface compressional modulus) will not be very reliable. However, comparing the K^s values for monolayers composed from the same lipid extracts on different subphases (Table 2) is possible. The trend for both pH 7.4 and 5.5 culture extracts measured on subphases buffered at pH 7.4 and 5.5, was the same for all of the *S. aureus* extracts tested, the K^s at pH 5.5 was higher than that obtained at pH 7.4. Only in the case of the pH 7.4 extract for MRSA G33, was this difference not statistically significant ($p > 0.05$, Mann–Whitney U test). This suggests that for all but one of the lipid extracts, acidifying the subphase reduces the elasticity of the monolayer.

The slope of the tangent to the isotherms at 40 mN/m (t_{40}) (Table 2), may provide a more reliable means of comparison between the extracts obtained for the same strains from different culture pHs, since this provides an indication of monolayer compressibility without taking into account the extrapolated area per molecule. A more negative t_{40} value indicates a steeper tangent and therefore a more condensed (less compressible) monolayer. When the t_{40} values for each extract on the different subphases were compared, the same trend observed for the K^s was found, whereby for all but the MRSA G33 pH 7.4 extract, the values were significantly more negative ($p < 0.05$, Mann–Whitney U test) for the pH5.5 subphase than for the one at pH 7.4. Comparing the t_{40} of the different extracts from the same strains, showed that for *S. aureus* 476 and MRSA strains G32 and H66, the pH 5.5 extracts on pH 5.5 subphase, were significantly more condensed than the pH 7.4 extracts on pH 7.4 subphase ($p < 0.05$, Mann–Whitney U test), both MRSA strains G33 and H64 showed no significant difference between the t_{40} values ($p > 0.05$, Mann–Whitney U test) of these two samples.

Analysis of each isotherm by plotting the first derivative (data not shown) revealed the presence of a transition point which we have considered to represent the onset of the transition between the liquid expanded and liquid condensed phases of the isotherms (LE/LC transition) (Figure 3, Table 2). For each of the extracts, with the exception of MRSA G33, the LE/LC transition occurs at a lower surface pressure on the pH 5.5 subphase than it does on pH 7.4 subphase. This again suggests that for *S. aureus* 476 and MRSA strains G32, H64 and H66, a modest monolayer condensing effect occurs when the subphase is acidified. Again, with the exception of MRSA G33, the greatest difference in LE/LC transition pressure was observed between the pH 7.4 extracts on a pH 7.4 subphase, and pH 5.5 extracts on a pH 5.5 subpahse.

3.3 Zeta potential measurements on *S. aureus* polar lipid extract vesicles

The MLVs formed from the pH 7.4 *S. aureus* lipid extracts exhibited highly negative zeta potentials (between -50 to -70 mV) in pH 7.4 buffer (Table 2). However, when the pH 7.4 lipid extracts were dispersed as MLVs in a pH 5.5 buffer, there was a significant shift of ~10 mV to a less negative zeta potential compared to the pH 7.4 buffer ($p < 0.05$, Mann-Whitney U test). Similar treatment of lipids extracted from bacteria cultured at pH 5.5 yielded differences between the zeta potentials in pH 7.4 and pH 5.5 buffers which were highly dependent upon the proportion of L-PG found in each extract (Table 2). The zeta potentials for the pH 5.5 MRSA G33 extract MLVs, which showed little difference in lipid composition between the two extracts (~30% L-PG in both cases), were found not to be significantly different ($p < 0.05$, Mann-Whitney U test) from those obtained from pH 7.4 extracts in both buffers. This was in marked contrast to the results observed for *S. aureus* 476 and MRSA strains G32 and H66 pH 5.5 extracts, all of which had L-PG contents >50% total phospholipid, which exhibited positive zeta potentials in the mildly acidic buffer. The MRSA H64 pH 5.5 lipid extract MLVs (~44% L-PG content) were effectively neutralized (~ -3 mV) in the pH 5.5 buffer.

3.4 Subphase injection of magainin 2 antimicrobial peptide

Injection of the antimicrobial peptide magainin 2 F5W into the subphase beneath monolayers formed from *S. aureus* 476 polar lipid extracts held at a fixed area, gives rise to an increase in surface pressure ($\delta\Pi$) which is indicative of partitioning of the peptide into the monolayer (Figure 4) (Maget-Dana, 1999). The kinetics of magainin 2 F5W adsorption at the interface (Table 3) is therefore dependent upon the affinity of the peptide for the pre-adsorbed lipid monolayer. Although the kinetic parameters obtained from the Gompertz function fits (Figure 3) show a high degree of variability (Table 3), this is most likely a result of the relatively large subphase volume through which the peptide had to diffuse. Nevertheless, the values for the maximum change in surface pressure ($\delta\Pi_{max}$) are consistent for each sample and clearly show that both monolayer composition and subphase pH greatly affect the degree of peptide adsorption.

For lipid extracts obtained from bacteria cultured at both pH 7.4 and pH 5.5, reducing the pH of the subphase leads to a decrease in $\delta\Pi_{max}$. In the case of the pH 7.4 extract, acidification of the subphase has little effect on the rate of surface pressure increase (k = 0.005 s^{-1} in both subphases) but, in addition to a slight attenuation of peptide affinity ($\delta\Pi_{max}$ reduced by ~2 mN/m), there is a noticeable lag in the onset of the partitioning (t_i occurs later). For the pH 5.5 extract, acidification of the subphase has a greater effect on peptide affinity ($\delta\Pi_{max}$ reduced by ~8.5 mN/m compared to the pH 7.4 extract at neutral pH) and although the rate of partitioning is markedly reduced (k = 0.013 s^{-1}), the interaction reaches equilibrium relatively quickly (t_i occurs earliest). These results clearly indicate that an increased L-PG content of the monolayer (in pH 5.5 extracts) together with the interfacial charge alteration which is likely to occur at the lower pH lead to a significant attenuation of the partitioning capability of magainin 2 F5W.

3.5 Neutron diffraction of *S. aureus* lipid extracts

The neutron diffraction profiles for fully hydrated (~100% RH) *S. aureus* 476 polar lipid extracts from both pH 7.4 and pH 5.5 cultures (Figure 5 and Supporting Information) could be indexed as lamellar phases, with a d-repeat spacing of 63.1 Å, which is similar to the repeat spacing previously measured by X-ray diffraction for *Escherichia coli* polar lipid extracts at the same temperature (~60 Å) (Staudegger et al., 2000).

In order to obtain more detail of the bilayer structure, SLD profiles of the bilayers from the pH 5.5 and 7.4 lipid extracts at ~100% humidity, were constructed as described in the Methods section. The resolution of SLD profiles is highly dependent on the number of orders of diffraction measured, and in both lipid extracts a maximum of three diffraction orders were detected therefore giving rise to SLD profiles of relatively low resolution, which can nevertheless yield useful estimates of bilayer thicknesses (Rappolt, 2010). Such low-resolution SLD profiles are typical of the L_α phase which contains lipids with high mobility, leading to reduction in the amount of coherent scattering (Pabst et al., 2010).

The SLD profiles of both pH 5.5 and 7.4 lipid extracts (Figure 5 insets) show that both bilayers were of comparable thickness (measured from the distance between the two, symmetrical positive SLD maxima). The hydrocarbon regions (the symmetrical regions either side of the zero on x axis which denotes the centre of the bilayer) of both bilayers had a thickness of ~26 Å, which is consistent with the dominant hydrocarbon chain species in each extract being branched C15 fatty acids (Singh *et al*., 2008). The SLD of the hydrocarbon regions of both pH lipid extracts were similar across the whole span of the hydrocarbon core and suggested both bilayers existed with a similar lateral density. The thicknesses of the headgroup regions of both lipid extract bilayers were estimated to be ~8-9 Å (Figure 5 insets) making them consistent with a mean headgroup thickness consisting of L-PG (10-12 Å), PG (6-7 Å) and CL (~7-8 Å) (as estimated from molecular densities) (Armen *et al*., 1998; Pascher et al., 1987) in both bilayers. This headgroup thickness was also consistent with previous findings suggesting that the L-PG headgroup existed in a loop structure due to an internal ionic bond between its protonated ε-amine and its phosphate group (El Mashak and Tocanne, 1979).

Co-deposition of the magainin 2 F5W peptide with the *S. aureus* 476 lipid extract bilayers facilitated differences in the responses of the pH 7.4 and pH 5.5 extracts. The pH 7.4 extract bilayers exhibited a decrease in d-spacing of 4.6 Å and a marked reduction in the intensity of the first order Bragg reflection (Figure 5), which may be indicative of increased bilayer disorder (Staudegger *et al*., 2000). Whilst the pH 5.5 extract bilayers exhibited a 3.1 Å reduction in d-spacing as a result of peptide addition, together with a small reduction in first order Bragg reflection intensity. The peak-to-peak distances of the SLD profiles (Figure 5 insets) suggest that the pH 7.4 extract bilayer reduces in thickness from ~47 Å to ~43 Å upon addition of the peptide. The pH 5.5 extract bilayers also decrease in thickness in response to peptide addition, from ~47 Å to ~44 Å.

In the co-deposited samples both the magainin 2 F5W and the bacterial lipid extracts were hydrogenated and therefore provided little in the way of the SLD contrast necessary to localise the peptide in relation to the density profile of the lipid bilayers (Figure 5 insets). Nevertheless, the differences apparent in the SLD profiles for both lipid extracts upon mixing with the peptide were of sufficient magnitude to allow us to estimate the regions of the bilayer containing the peptide. The difference profile shown alongside the SLD profiles for bilayers in the absence and presence of peptide clearly illustrate the density changes across the bilayer normal elicited by the presence of magainin 2 F5W. For the pH 7.4 lipid extract sample, the density changes observed upon peptide addition may indicate that it resides both in the headgroup regions and in the hydrophobic core of the bilayers. This is in marked contrast to the pH 5.5 extract bilayers, which show only very small density changes in the headgroup regions and no peptide in the bilayer core.

4 Discussion

Despite the fact that culture pH has been known to stimulate the biosynthesis of L-PG in *S. aureus* for almost five decades (Gould and Lennarz, 1970) the physiological significance of this phenomenon has become somewhat neglected. Most recent research has focused on the genetic regulation and role of the lysyl-transferase MprF (responsible for L-PG biosynthesis) in resistance to host defensins, other antimicrobial peptides and lipopeptides (Li *et al*., 2007; Mukhopadhyay *et al*., 2007; Nishi *et al*., 2004; Yang *et al*., 2009). However, these factors form part of a number of concomitant and overlapping stressors, which threaten *S. aureus* in its environmental niche as a human commensal, and thus have important implications for its ability to colonise and cause pathology in certain hosts. The epidermis and mucosal surfaces which are commonly colonised by *S. aureus* are rich in defensive peptides and are characterised by their mild acidity (Arendt *et al*., 2012), both of which serve as innate defences against pathogenic bacteria. The fact that biosynthesis of bacterial aminoacyl-phosphatidylglycerols such as L-PG is stimulated by these and other mucosal defences (Arendt *et al*., 2012), serves to reinforce the importance of studying the mechanism whereby these lipids may facilitate bacterial survival. Whereas most publications have speculated that increased L-PG mediates resistance to membrane-active antimicrobials by neutralising membrane charge (Roy, 2009) through the formation of lipid ion-pairs, the evidence of this study points to a more nuanced picture of L-PG's role in defending membrane integrity.

From the phospholipid extracts we examined by ^{31}P NMR, the observation that in neutral pH growth medium all five *S. aureus* strains contained ~30% L-PG is 2 to 10 times higher than has been reported in other recent studies (Mukhopadhyay *et al*., 2007; Nishi *et al*., 2004), but is consistent with those previously reported for *S. aureus* grown in glucose-containing basal media (Gould and Lennarz, 1970). These apparent discrepancies in the detected proportions of L-PG in *S. aureus* membranes can be attributed to a number of factors, including the influence of culture media ingredients (Gould and Lennarz, 1970), and the necessity to acidify extraction solvents in order to prevent hydrolysis of the alkali-labile L-PG (Foreman-Wykert *et al*., 2000). The fact that previous studies have relied on thin layer chromatography using alkaline solvents (Mukhopadhyay *et al*., 2007; Nishi *et al*., 2004) to analyse the content of *S. aureus* lipid extracts, would certainly lead to low estimates of L-PG content being reported, due to hydrolysis of the lipid during analysis (Danner *et al*., 2008). In our study, culture at pH 5.5 elicited an increase in L-PG biosynthesis in all of the strains tested, some of which showed amounts increase to ~50% of total phospholipid. Less impressive increases in L-PG content were detected in strains G33 and H64, which may be expected since *mprF* polymorphism is known to occur in clinical strains of MRSA and leads to markedly different rates of L-PG biosynthesis (Yang *et al*., 2009). The acid-induced increase in levels of L-PG which we observed was not only consistent with previous findings (Gould and Lennarz, 1970) but was corroborated by the zeta potential and air/liquid monolayer characterisation conducted on the lipid extracts.

The theorised tandem effects of charge dampening and increased ordering in membranes with higher L-PG content (Roy, 2009) were both effectively

demonstrated following the analysis of *S. aureus* extracts by zeta potential and air/liquid interface monolayer isotherms. However, there is one very important caveat, evident from our results, which is that increased L-PG alone does not significantly affect the membrane charge although it does seem to be important for altering the ordering of lipid monolayers. Both of these properties appear to be highly dependent upon the ionisation state of the L-PG headgroup, in addition to the amount of the lipid present. With respect to the zeta potential measurements, assuming that the lipid distribution in the extract vesicles was symmetric across both leaflets, the results obtained appear unequivocal. The zeta potentials of the reconstituted *S. aureus* lipid membranes are only effectively neutralised when the proportion of L-PG is greater than 44% and the bulk pH is reduced from 7.4 to 5.5, since only these fall within the ±20 mV range indicative of particle neutrality (Clogston and Patri, 2011). This neatly demonstrates the importance of the ionisation state of the L-PG headgroup α-amine (pK_a ~7.0) in facilitating the membrane lipid ion-pairing thought to be in part responsible for antimicrobial peptide resistance in *S. aureus* and other bacteria. A similar pattern of results was observed in the results of the Langmuir monolayer data. These experiments were designed to detect any changes in lipid ordering, by examining the effects of L-PG content on the surface compressibility moduli and LE/LC phase onset in the lipid extract monolayers. Although there is some intra-strain consistency in the compressibility modulus data, which suggests that decreasing the subphase pH and thus the proportion of ion-paired lipids, increases the rigidity of the monolayers, the inter-strain results are not comparable. This most likely results from inaccuracies in the estimated average molecular weights of the lipids due to the presence of fluctuating amounts of impurities within the different batches of bacterial lipid extracts. Conversely, the LE/LC phase onset results are independent of the average molecular weight and are thus comparable between the different strains. These data show a clear relationship between L-PG content at the surface pressure at which the LE/LC phase begins. The general trend of both increased L-PG and decreased pH eliciting onset of the LE/LC transition at lower surface pressures, probably indicates that a modest monolayer ordering effect is facilitated by both of these factors.

Having thus established the enhancing effect of mild acidity on both L-PG biosynthesis and its ability to alter membrane properties through ion-pairing, in different bacterial strain lipid extracts, the effect of L-PG on antimicrobial peptide activity was studied exclusively with *S. aureus* 476 lipids. Subphase injection of the amphibian AMP mutant magainin 2 F5W offered a convenient way to assess the ability of the peptide to penetrate into lipid monolayers (Maget-Dana, 1999) under different conditions of pH and L-PG content. Indeed this technique has recently been employed to demonstrate that a mildly acidic subphase pH enhances the penetration of an anionic amphiphilic peptide into model *S. aureus* lipid monolayers containing synthetic lysyl-DOPG (Dennison *et al*., 2016). Our approach has been to analyse the kinetics of peptide-monolayer interactions in order to go beyond commonly employed qualitative descriptions of the data (Hubbard *et al*., 2017). From the data obtained, the interaction impeding and attenuating effects are evident, whereby increasing the monolayer L-PG content and decreasing the subphase pH acted synergistically to impressively reduce peptide penetration. Indeed the very small magnitude (δΠ ~2

mN/m) of the surface pressure increase seen upon injection of the peptide under *S. aureus* 476 lipid monolayers from pH 5.5 extracts on a pH 5.5 subphase are indicative of some small headgroup interactions and little or no intercalation into the lipid layer (Demel *et al*., 1973). This would appear to corroborate a previous study into *S. aureus* antimicrobial peptide resistance, which used synthetic L-PG-containing liposomes and concluded that increased L-PG did not attenuate peptide-membrane interactions, but did prevent membrane lysis (Kilelee *et al*., 2010). However, a more appropriate comparison between that study and ours required the more detailed analysis of the peptide interaction obtained from our neutron diffraction measurements.

Partitioning of Magainin 2 is known to cause significant thinning of synthetic bacterial membranes, by ~2.5 Å at 92% RH, which was suggested to occur when peptide residing at the interfacial region increased lipid chain disorder (Ludtke *et al*., 1995). With our natural lipid extracts under similar conditions (with 2 mol% peptide in contrast to 1.5% (Ludtke *et al*., 1995) and ~100% RH) a maximal magainin-induced bilayer thinning of 3.4 Å was observed in the pH 7.4 extract sample (~30% L-PG). Increasing the amount of L-PG to over 50% (in the pH 5.5 extract) elicited a slight reduction in tinning, to 2.1 Å and reduced the amount of bilayer disorder elicited by the presence of the peptide. Evidence from the SLD profiles suggests that although the increased L-PG excluded more of the peptide from the hydrophobic core of the bilayers, it remained associated with the headgroups (Figure 6), a conclusion seemingly consistent with results obtained from studying the lytic activity of peptides against L-PG-containing vesicles (Andra *et al*., 2011; Kilelee *et al*., 2010) and from the monolayer partitioning results obtained in this study. However, the lack of pH control in the neutron diffraction studies should be borne in mind when comparing these data with previous studies. The apparent decrease in peptide penetration may result purely from reduced affinity due to an increase in the amount of neutral lipid present, and not as a result of L-PG-mediated repulsion. As our peptide-monolayer interaction data shows, simply increasing the amount of L-PG at neutral pH, is enough to significantly attenuate peptide partitioning, but it requires full ionisation of L-PG to trigger its full membrane-defensive potential.

When discussing the validity of any data obtained using natural or synthetic L-PG, consideration of its alkali-lability is imperative. Although the experiments described in this paper were designed to minimise both chemical and physical stresses on the lipid, it is inevitable that any handling would result in some degree of hydrolysis (Campbell, 1982; Danner *et al*., 2008). Although our extraction and analysis techniques negated the use of neutral or alkaline solvents (Mukhopadhyay *et al*., 2007; Nishi *et al*., 2004) which would have resulted in underestimation of L-PG content and our sample preparation avoided the use of sonication (Andra *et al*., 2011; Kilelee *et al*., 2010) which would undoubtedly destroy L-PG, our results must however be viewed with at least some caution. Having said that we nevertheless believe that this study provided compelling evidence for the importance of mild acidity in both enhancing L-PG biosynthesis and facilitating its membrane-protective functions of charge dampening and increasing rigidity.

The data presented here shed some light on how L-PG might play a role in both survival of *S. aureus* during colonisation and even infection of its human host. In its commensal niche and its virulent state, *S. aureus* is able to survive on body surfaces and within intracellular compartments which are both mildly acidic and rich in antimicrobial peptides (Arendt *et al*., 2012; Gresham *et al*., 2000; Peschel *et al*., 2001), two factors known to trigger increased L-PG biosynthesis (Gould and Lennarz, 1970; Li *et al*., 2007). Even in strains which produce lower amounts of L-PG in response to such stimuli, such as the MRSA G33 used in this study, protective levels in the outer leaflet of the plasma membrane could be maintained by the MprF flopase sub-unit which facilitates its asymmetric distribution (Ernst and Peschel, 2011). The presence of a higher proportion of L-PG on the cell membrane outer leaflet not only facilitates its function, but also protects it from degradation due to the mild acidity naturally maintained in that region of the cell envelope (Collins and Hamilton, 1976). All of which further reinforces the vital importance of considering pH in any future research into the role of L-PG in *S. aureus* and other bacteria.

Acknowledgements

The authors wish to thank Professor Jonathan Edgeworth of the CIDR at Guy's and St. Thomas' NHS Foundation Trust Hospital in London, for the generous donation of the *S. aureus* clinical isolate strains used in this study. The ILL is acknowledged for the allocation of beam-time and use of laboratory preparation facilities within the PSCM. Special thanks go to Dr Damian Rivett of Imperial College London for his invaluable discussions and support throughout this research. RPR was financially supported by the Biotechnology and Biological Sciences Research Council (UK). HM was financially supported by a King's College London Health Schools Studentship. ATMH was financially supported throughout this study by a studentship from St George's, University of London. RDH was financially supported by a Next Generation Facility Users Grant (EP/G068569/1) from the Engineering and Physical Sciences Research Council (UK).

Tables and Figures

[a]Based on multi-locus sequence typing genetic fingerprinting.
[b]Based on the sequence of the polymorphic region of the Protein A gene.
[c]The minimum inhibitory concentration.

[a]Slope of the tangent to the isotherm at 40 mN/m.
[b]Surface compressional modulus measured at 40 mN/m.
[C]Determined from the first derivative of the pressure-area isotherm.
[d]Zeta potential.

Figure 1. Representative chemical structures of the three mail phospholipids found in the plasma membrane of *S. aureus*, phosphatidylglycerol (PG), cardiolipin (CL) and lysyl-phosphatidylglycerol (L-PG).

Figure 2. Phosphorous NMR spectra of (A) CL, PG and L-PG synthetic lipid standards and (B) *S. aureus* 476 polar lipid extract, showing the chemical shifts for the three main phospholipid components.

Figure 3. Langmuir monolayer isotherms (23°C) of *S. aureus* polar lipid extracts from bacteria (Black – *S. aureus* 476, Red – MRSA G32, Blue – MRSA G33, Orange – MRSA H64, Purple – MRSA H66) cultured at either pH 7.4 (A and B) or pH 5.5 (C and D). For each extract, the isotherms were obtained on subphases containing 10 mM Tris–acetate buffer adjusted to either pH 7.4 (A and C) or pH 5.5 (B and D). On each graph the grey line indicates the surface pressure of the onset of the LE/LC transition for MRSA G32, determined from the first derivative of the isotherm.

Figure 4. The kinetics of magainin 2 F5W partitioning into *S. aureus* 476 lipid extract monolayers at different extract and subphase pHs measured at 23°C, at a lipid/peptide molar ratio of 1:1.2. The data points were obtained from single representative measurements and were fitted with a sigmoidal Gompertz function.

Figure 5. Raw neutron diffraction profiles for *S. aureus* 476 lipid extracts from bacteria cultured at (A) pH 7.4 and (B) pH 5.5, in the absence (blue lines) and presence (red lines) of the antimicrobial peptide magainin 2 F5W (lipid/peptide molar ratio of 50:1), measured at 25°C and 100% RH in D_2O. The highlighted section shows the third order diffraction peak (multiplied 10 times) for the lipid sample in the absence of peptide. The insets show the relative scattering length density profiles across the bilayers (in the z axis perpendicular to the bilayer plane) in the absence (blue lines) and presence (red lines) of antimicrobial peptide together with a difference profile (black lines) showing the effect of magainin 2 F5W addition.

Figure 6. Representations of the possible relationships between magainin 2 F5W and *S. aureus* 476 lipid extracts from bacteria cultured at (A) pH 7.4 and (B) pH 5.5 in the co-deposited samples prepared for neutron diffraction measurements. The yellow lipid headgroups represent those of PG or CL (anionic) and the green headgroups represent those of L-PG in two charge states: zwitterionic (light green) and cationic (dark green). The neutron diffraction data (Figure 5) suggest that there was a deeper peptide penetration of the bilayers composed of pH 7.4 extracts, whereas the peptide was mainly localised at the interfacial region in pH 5.5 extract bilayers.

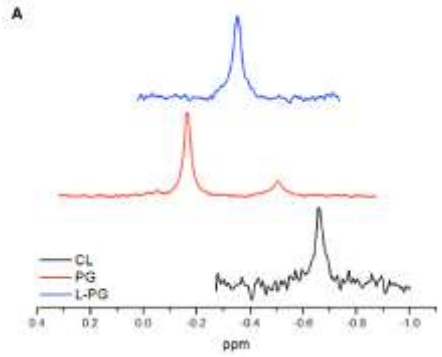

<InlineImage3>

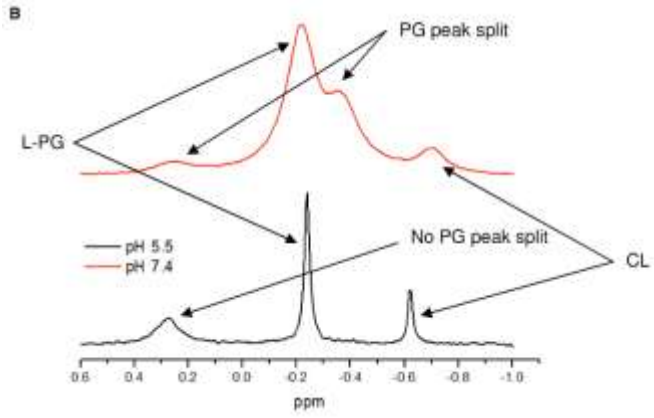

<InlineImage4>

Figure 2

References

Andra, J., Goldmann, T., Ernst, C.M., Peschel, A., Gutsmann, T., 2011. Multiple Peptide Resistance Factor (MprF)-mediated Resistance of Staphylococcus aureus against Antimicrobial Peptides Coincides with a Modulated Peptide Interaction with Artificial Membranes Comprising Lysyl-Phosphatidylglycerol. Journal of Biological Chemistry 286, 18692-18700.

Arendt, W., Hebecker, S., Jager, S., Nimtz, M., Moser, J., 2012. Resistance Phenotypes Mediated by Aminoacyl-Phosphatidylglycerol Synthases. Journal of Bacteriology 194, 1401-1416.

Armen, R.S., Uitto, O.D., Feller, S.E., 1998. Phospholipid component volumes: Determination and application to bilayer structure calculations. Biophysical Journal 75, 734-744.

Bligh, E.G., Dyer, W.J., 1959. A rapid method of total lipid extraction and purification. Canadian Journal of Biochemistry and Physiology 37, 911-917.

Bucki, R., Pastore, J.J., Randhawa, P., Vegners, R., Weiner, D.J., Janmey, P.A., 2004. Antibacterial Activities of Rhodamine B-Conjugated Gelsolin-Derived Peptides Compared to Those of the Antimicrobial Peptides Cathelicidin LL37, Magainin II, and Melittin. Antimicrobial Agents and Chemotherapy 48, 1526-1533.

Buldt, G., Gally, H., Seelig, J., Zaccai, G., 1979. Neutron-Diffraction Studies on Phosphatidylcholine Model Membranes .1. Head Group Conformation. Journal of Molecular Biology 134, 673-691.

Campbell, P.I., 1982. *Staphylococcus aureus* lysyl-phosphatidylglycderol an unsuitable adjunct for preparing cationic liposomes. Microbios Letters 19, 11-16.

Clogston, J.D., Patri, A.K., 2011. Zeta potential measurement. Methods in molecular biology 697, 63-70.

Collins, S.H., Hamilton, W.A., 1976. Magnitude of the protonmotive force in respiring Staphylococcus aureus and Escherichia coli. Journal of bacteriology 126, 1224-1231.

Cox, E., Michalak, A., Pagentine, S., Seaton, P., Pokorny, A., 2014. Lysylated phospholipids stabilize models of bacterial lipid bilayers and protect against antimicrobial peptides. Biochimica et Biophysica Acta (BBA)-Biomembranes.

Danner, S., Pabst, G., Lohner, K., Hickel, A., 2008. Structure and thermotropic behavior of the Staphylococcus aureus lipid lysyl-dipalmitoylphosphatidylglycerol. Biophysical Journal 94, 2150-2159.

Demel, R.A., London, Y., Geurts van Kessel, W.S., Vossenberg, F.G., van Deenen, L.L., 1973. The specific interaction of myelin basic protein with lipids at the air-water interface. Biochim Biophys Acta 311, 507-519.

Denich, T.J., Beaudette, L.A., Lee, H., Trevors, J.T., 2003. Effect of selected environmental and physico-chemical factors on bacterial cytoplasmic membranes. Journal of microbiological methods 52, 149-182.

Dennison, S.R., Morton, L.H., Harris, F., Phoenix, D.A., 2016. Low pH Enhances the Action of Maximin H5 against Staphylococcus aureus and Helps Mediate Lysylated Phosphatidylglycerol-Induced Resistance. Biochemistry 55, 3735-3751.

Dynarowicz-Latka, P., Hac-Wydro, K., 2004. Interactions between phosphatidylcholines and cholesterol in monolayers at the air/water interface. Colloids and surfaces. B, Biointerfaces 37, 21-25.

El Mashak, E.M., Tocanne, J.F., 1979. A monolayer study of the adsorption of methyl-lysine at phosphatidylglycerol-water interfaces: A model for elucidating the conformation of the Lisylphosphatidylglycerol polar head. Journal of Colloid and Interface Science 70, 56-66.

Ernst, C.M., Peschel, A., 2011. Broad-spectrum antimicrobial peptide resistance by MprF-mediated aminoacylation and flipping of phospholipids. Molecular Microbiology 80, 290-299.

Foreman-Wykert, A.K., Weiss, J., Elsbach, P., 2000. Phospholipid synthesis by Staphylococcus aureus during (Sub)Lethal attack by mammalian 14-kilodalton group IIA phospholipase A2. Infect Immun 68, 1259-1264.

Gaines, G.L., 1966. Insoluble monolayers at liquid-gas interfaces. Interscience, New York ; London, etc.

Gould, R.M., Lennarz, W.J., 1970. Metabolism of phosphatidylglycerol and lysyl phosphatidylglycerol in *Staphylococcus aureus*. Journal of Bacteriology 104, 1135 - 1144.

Gresham, H.D., Lowrance, J.H., Caver, T.E., Wilson, B.S., Cheung, A.L., Lindberg, F.P., 2000. Survival of Staphylococcus aureus inside neutrophils contributes to infection. Journal of immunology 164, 3713-3722.

Haines, T.H., 2009. A new look at Cardiolipin. Bba-Biomembranes 1788, 1997-2002.

Hornef, M.W., Normark, S., Henriques-Normark, B., Rhen, M., 2005. Bacterial evasion of innate defense at epithelial linings. Chem Immunol Allergy 86, 72-98.

Hubbard, A.T., Barker, R., Rehal, R., Vandera, K.A., Harvey, R.D., Coates, A.R., 2017. Mechanism of Action of a Membrane-Active Quinoline-Based Antimicrobial on Natural and Model Bacterial Membranes. Biochemistry 56, 1163-1174.
Khatib, T.O., Stevenson, H., Yeaman, M.R., Bayer, A.S., Pokorny, A., 2016. Binding of Daptomycin to Anionic Lipid Vesicles Is Reduced in the Presence of Lysyl-Phosphatidylglycerol. Antimicrob Agents Chemother.
Kilelee, E., Pokorny, A., Yeaman, M.R., Bayer, A.S., 2010. Lysyl-Phosphatidylglycerol Attenuates Membrane Perturbation Rather than Surface Association of the Cationic Antimicrobial Peptide 6W-RP-1 in a Model Membrane System: Implications for Daptomycin Resistance. Antimicrobial Agents and Chemotherapy 54, 4476-4479.
Lad, M.D., Birembaut, F., Clifton, L.A., Frazier, R.A., Webster, J.R.P., Rebecca J. Green, R.J., 2007. Antimicrobial Peptide-Lipid Binding Interactions and Binding Selectivity. Biophysical Journal 92, 3575-3586.
Leonard, A., Escrive, C., Laguerre, M., Pebay-Peyroula, E., Neri, W., Pott, T., Katsaras, J., Dufourc, E.J., 2001. Location of cholesterol in DMPC membranes. A comparative study by neutron diffraction and molecular mechanics simulation. Langmuir 17, 2019-2030.
Li, M., Cha, D.J., Lai, Y., Villaruz, A.E., Sturdevant, D.E., Otto, M., 2007. The antimicrobial peptide-sensing system aps of Staphylococcus aureus. Molecular Microbiology 66, 1136-1147.
Ludtke, S., He, K., Huang, H., 1995. Membrane thinning caused by magainin 2. Biochemistry 34, 16764-16769.
Maget-Dana, R., 1999. The monolayer technique: a potent tool for studying the interfacial properties of antimicrobial and membrane-lytic peptides and their interactions with lipid membranes. Biochimica et Biophysica Acta (BBA)-Biomembranes 1462, 109-140.
Mukhopadhyay, K., Whitmire, W., Xiong, Y.Q., Molden, J., Jones, T., Peschel, A., Staubitz, P., Adler-Moore, J., McNamara, P.J., Proctor, R.A., Yeaman, M.R., Bayer, A.S., 2007. In vitro susceptibility of Staphylococcus aureus to thrombin-induced platelet microbicidal protein-1 (tPMP-1) is influenced by cell membrane phospholipid composition and asymmetry. Microbiology-Sgm 153, 1187-1197.
Nesbitt, J.A., Lennarz, W.J., 1968. Participation of aminoacyl transfer ribonucleic acid in aminoacyl phosphatidylglycerol synthesis. I. Specificity of lysyl phosphatidylglycerol synthetase. Journal of Biological Chemistry 243, 3088-&.
Nishi, H., Komatsuzawa, H., Fujiwara, T., McCallum, N., Sugai, M., 2004. Reduced content of lysyl-phosphatidylglycerol in the cytoplasmic membrane affects susceptibility to moenomycin, as well as vancomycin, gentamicin, and antimicrobial peptides, in Staphylococcus aureas. Antimicrobial Agents and Chemotherapy 48, 4800-4807.
Pabst, G., Kucerka, N., Nieh, M.P., Rheinstadter, M.C., Katsaras, J., 2010. Applications of neutron and X-ray scattering to the study of biologically relevant model membranes. Chemistry and Physics of Lipids 163, 460-479.
Pascher, I., Sundell, S., Harlos, K., Eibl, H., 1987. Conformation and packing properties of membrane lipids: the crystal structure of sodium dimyristoylphosphatidylglycerol. Biochimica et Biophysica Acta (BBA)-Biomembranes 896, 77-88.
Pebaypeyroula, E., Dufourc, E.J., Szabo, A., 1994. Location of Diphenyl-Hexatriene and Trimethylammonium-Diphenyl-Hexatriene in Dipalmitoylphosphatidylcholine Bilayers by Neutron-Diffraction. Biophysical Chemistry 53, 45-56.
Perino-Gallice, L., Fragneto, G., Mennicke, U., Salditt, T., Rieutord, F., 2002. Dewetting of solid-supported multilamellar lipid layers. The European physical journal. E, Soft matter 8, 275-282.
Peschel, A., Jack, R.W., Otto, M., Collins, L.V., Staubitz, P., Nicholson, G., Kalbacher, H., Nieuwenhuizen, W.F., Jung, G., Tarkowski, A., 2001. Staphylococcus aureus resistance to human defensins and evasion of neutrophil killing via the novel virulence factor MprF is based on modification of membrane lipids with l-lysine. The Journal of experimental medicine 193, 1067-1076.
Rappolt, M., 2010. Bilayer thickness estimations with "poor" diffraction data. J Appl Phys 107.
Rehal, R., 2014. A Physicochemical and Biophysical Investigation into the Role of Lysyl-Phosphatidylglycerol in the Membrane of Staphylococcus aureus under mild acidic conditions., Institute of Pharmaceutical Science. King's College London, London.
Richard, D., Ferrand, M., Kearley, G.J., 1996. Analysis and Visualisation of Neutron-Scattering Data. Journal of Neutron Research 4, 33-39.
Roy, H., 2009. Tuning the Properties of the Bacterial Membrane with Aminoacylated Phosphatidylglycerol. Iubmb Life 61, 940-953.
Saxena, A.M., Schoenborn, B.P., 1977. Correction factors for neutron-diffraction from lamellar structures. Acta Crystallographica Section A 33, 813-818.

Sebastiani, F., Harvey, R., Khanniche, S., Artero, J.B., Haertlein, M., Fragneto, G., 2012. Diffraction studies on natural and model lipid bilayers. European Physical Journal-Special Topics 213, 355-365.
Singh, V.K., Hattangady, D.S., Giotis, E.S., Singh, A.K., Chamberlain, N.R., Stuart, M.K., Wilkinson, B.J., 2008. Insertional Inactivation of Branched-Chain α-Keto Acid Dehydrogenase in Staphylococcus aureus Leads to Decreased Branched-Chain Membrane Fatty Acid Content and Increased Susceptibility to Certain Stresses. Applied and Environmental Microbiology 74, 5882-5890.
Staubitz, P., Neumann, H., Schneider, T., Wiedemann, I., Peschel, A., 2004. MprF-mediated biosynthesis of lysylphosphatidylglycerol, an important determinant in staphylococcal defensin resistance. Fems Microbiology Letters 231, 67-71.
Staudegger, E., Prenner, E.J., Kriechbaum, M., Degovics, G., Lewis, R.N.A.H., McElhaney, R.N., Lohner, K., 2000. X-ray studies on the interaction of the antimicrobial peptide gramicidin S with microbial lipid extracts: evidence for cubic phase formation. Biochimica et Biophysica Acta (BBA) - Biomembranes 1468, 213-230.
Tocanne, J.F., Ververgaert, P.H.J.T., Verkleij, A.J., van Deenen, L.L.M., 1974. A monolayer and freeze-etching study of charged phospholipids I. Effects of ions and pH on the ionic properties of phosphatidylglycerol and lysylphosphatidylglycerol. Chemistry and Physics of Lipids 12, 201-219.
Winsor, C.P., 1932. The Gompertz Curve as a Growth Curve. Proceedings of the National Academy of Sciences of the United States of America 18, 1-8.
Worcester, D.L., Franks, N.P., 1976. Structural-analysis of hydrated egg lecithin and cholesterol bilayers. 2. Neutron diffraction. Journal of Molecular Biology 100, 359-378.
Yang, S.J., Xiong, Y.Q., Dunman, P.M., Schrenzel, J., Francois, P., Peschel, A., Bayer, A.S., 2009. Regulation of mprF in daptomycin-nonsusceptible Staphylococcus aureus strains. Antimicrob Agents Chemother 53, 2636-2637.

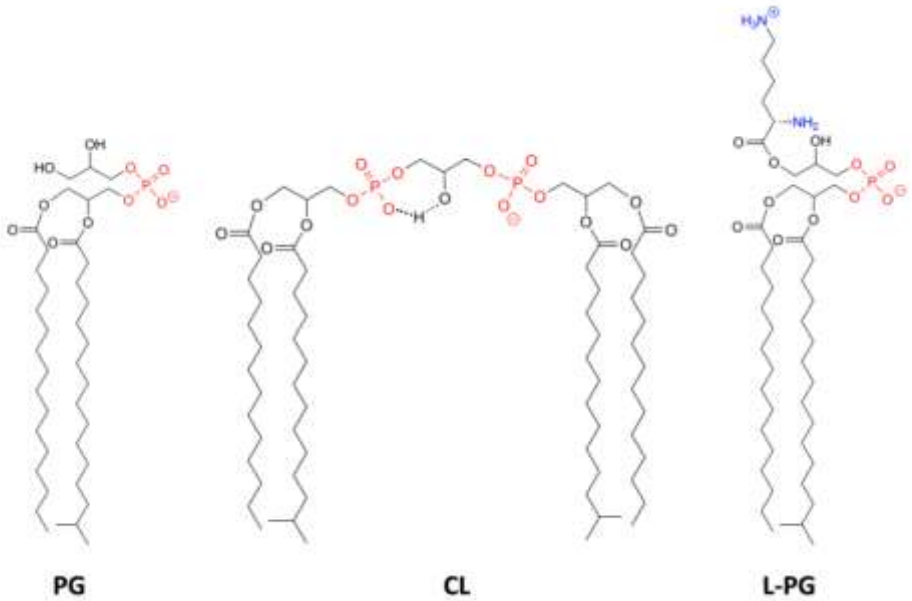

<InlineImage2>

Figure 1.

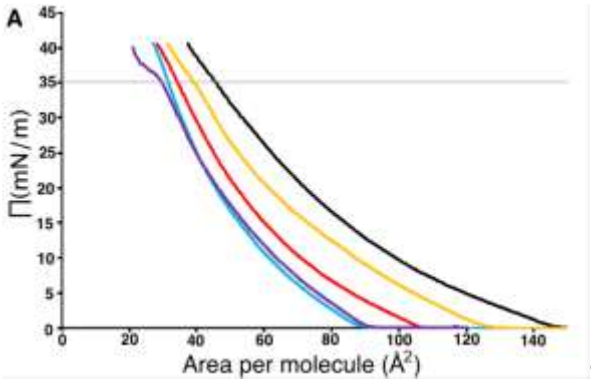

<InlineImage5>

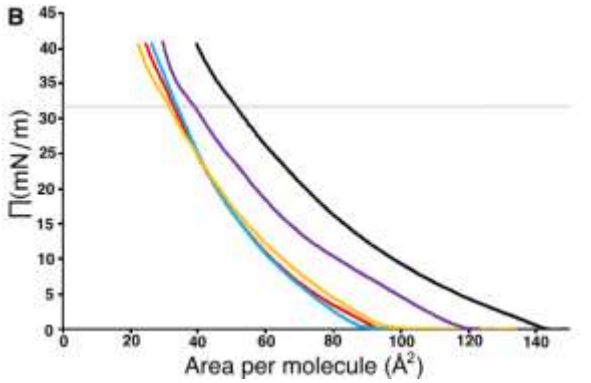

<InlineImage6>

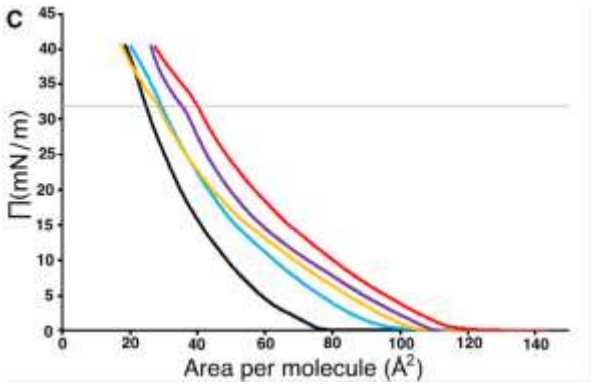

<InlineImage7>

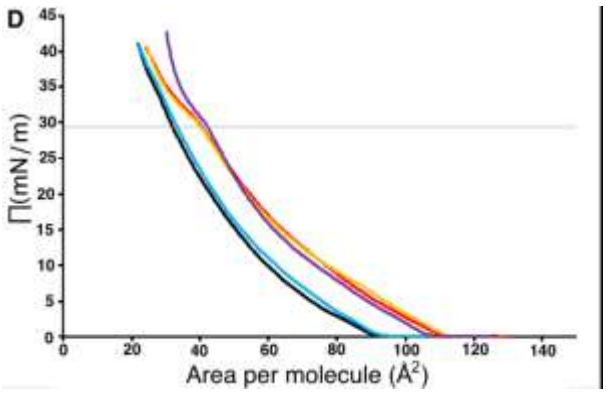

<InlineImage8>

Figure 3.

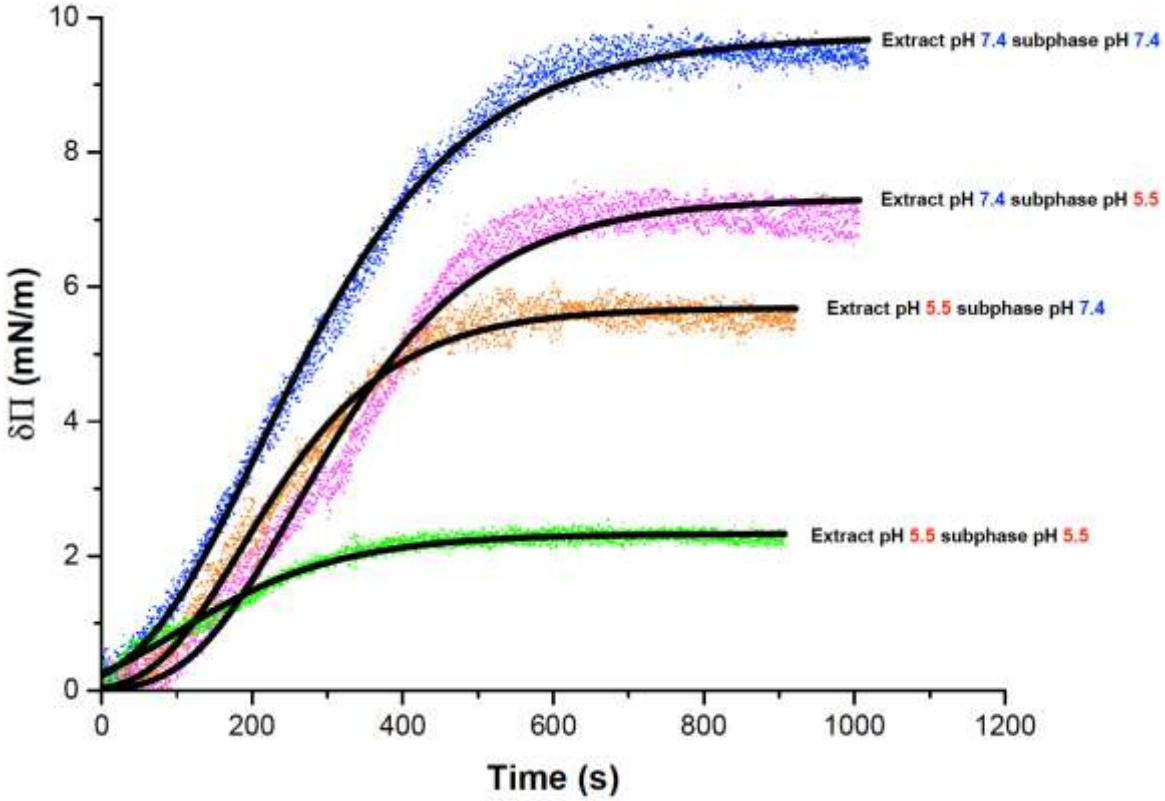

<InlineImage9>

Figure 4.

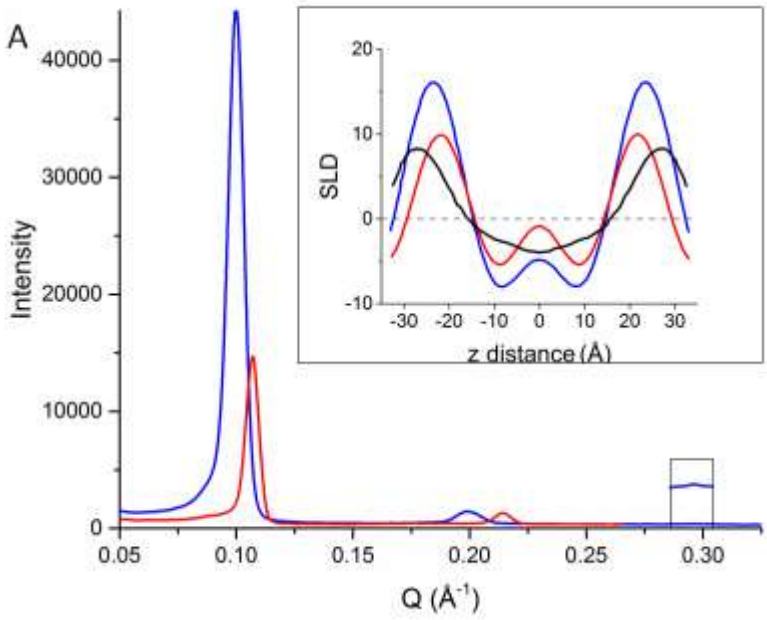

<InlineImage10>

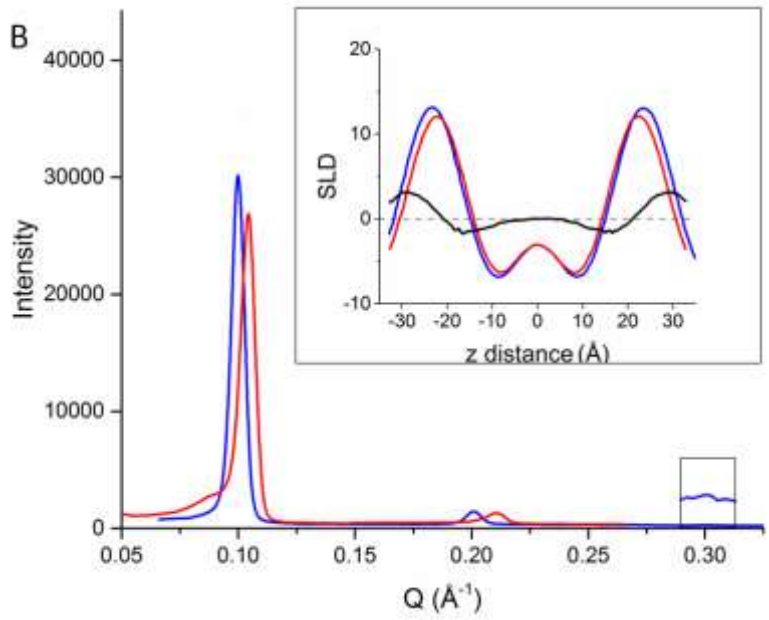

<InlineImage11>

Figure 5.

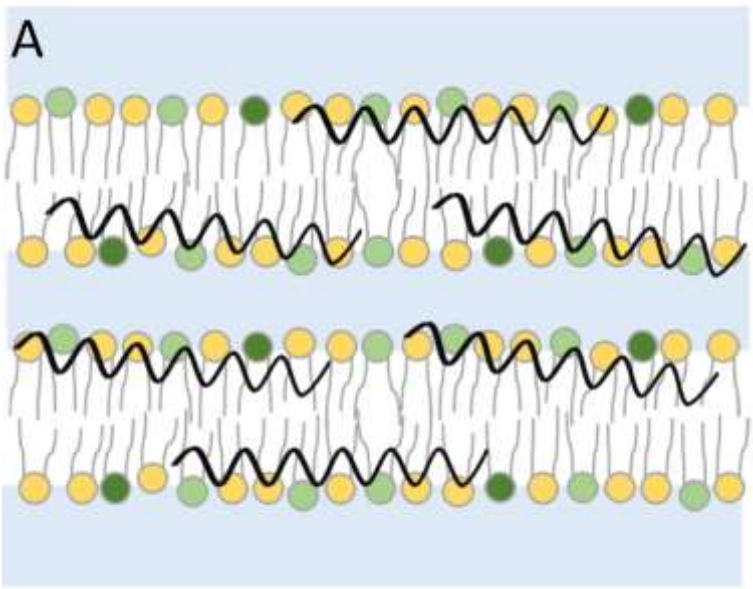

<InlineImage12>

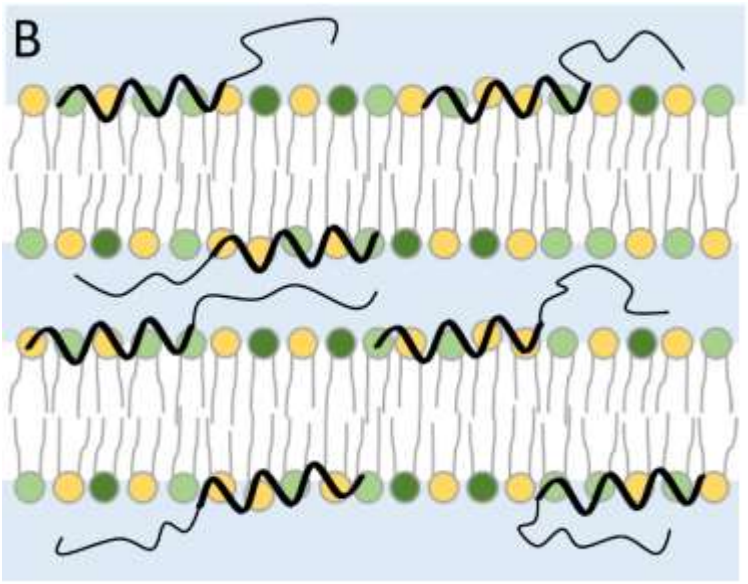

<InlineImage13>

Figure 6.

Table 1 Selected genotypic and phenotypic characteristics of the clinically-isolated *Staphylococcus aureus* strains used in this study.

Strain	Sequence type[a]	Spa type[b]	Vancomycin MIC[c] (μg/mL)
S. aureus 476	ST1	T183	<0.5
MRSA G32	ST239	T032	>1.5
MRSA G33	ST22	T032	<0.5
MRSA H64	ST36	T018	<0.5
MRSA H66	ST36	T018	<0.5

Table 2. The compositions and estimated average molecular weights of lipid extracts obtained from different *S. aureus* strains cultured at pHs 7.4 and 5.5, showing the effect of pH on the physical parameters obtained from pressure-area isotherms of air/liquid interface monolayers and the electrophoretic movement of reconstituted vesicles. All values are means obtained from triplicate samples.

Strain	pH		Lipid composition (%)				Monolayer parameters			Vesicles
	Extract	Bulk	PG	LPG	CL	M_w	t_{40} [a] (δΠ/δA)	K^s [b] (mN/m)	LE/LC[c] (mN/m)	ζ [d] (mV)
476	5.5	5.5	43 ± 4	51± 4	6 ± 2	887	-1.6 ± 0.1	76 ± 2	32	+17 ± 5
	5.5	7.4					-1.5 ± 0	67 ± 1	34	-43 ± 11
	7.4	5.5	62 ± 4	33 ± 4	4 ± 1	860	-1 ± 0.1	78 ± 0	32	-55 ± 7
	7.4	7.4					-0.8 ± 0	68 ± 0	35	-55 ± 10
G32	5.5	5.5	40 ± 3	52 ± 6	8 ± 3	900	-1 ± 0	63 ± 1	29	+21 ± 11
	5.5	7.4					-0.8 ± 0.1	61 ± 0	33	-37 ± 7
	7.4	5.5	67 ± 1	28 ± 4	5 ± 2	859	-1.2 ± 0.1	69 ± 1	33	-48 ± 10
	7.4	7.4					-1 ± 0.1	66 ± 0	35	-56 ± 12
G33	5.5	5.5	66 ± 6	28 ± 4	6 ± 2	868	-1.2 ± 0	66 ± 1	34	-51 ± 10
	5.5	7.4					-1 ± 0.1	61 ± 1	34	-60 ± 9
	7.4	5.5	58 ± 8	34 ± 10	9 ± 3	877	-1.2 ± 0	72 ± 0	35	-64 ± 12
	7.4	7.4					-1.1 ± 0	70 ± 3	36	-68 ± 10
H64	5.5	5.5	50 ± 4	44 ± 7	6 ± 2	879	-1.5 ± 0.2	75 ± 6	28	-4 ± 8
	5.5	7.4					-1 ± 0	57 ± 2	32	-44 ± 8
	7.4	5.5	64 ± 3	33 ± 3	4 ± 0	860	-1.3 ± 0.1	67 ± 3	32	-50 ± 11
	7.4	7.4					-0.9 ± 0.1	65 ± 2	34	-57 ± 10
H66	5.5	5.5	40 ± 6	55 ± 8	5 ± 7	877	-2.5 ± 0.4	113 ± 13	28	+15 ± 10
	5.5	7.4					-1.4 ± 0.1	74 ± 5	30	-46 ± 17
	7.4	5.5	61 ± 7	34 ± 9	5 ± 1	866	-1.7 ± 0.1	88 ± 2	31	-56 ± 14
	7.4	7.4					-1 ± 0.1	62 ± 2	35	-62 ± 12

Table 3. Kinetic parameters obtained from Gompertz function fitting of pressure-time isotherms for *S. aureus* 476 lipid extract monolayers held at a fixed area, after subphase injection of magainin 2 F5W on an aqueous subphase containing 10 mM Tris-acetate buffer adjusted to pH 7.4 or 5.5. The values shown are means from three independent measurements, together with their standard deviations.

Culture pH	Subphase pH	$\delta\Pi_{max}$ (mN/m)	t_i (s)	k (s^{-1})
5.5	5.5	2 ± 0	74 ± 22	0.013 ± 0.005
	7.4	6 ± 1	195 ± 74	0.007 ± 0.002
7.4	5.5	8 ± 1	329 ± 72	0.005 ± 0.002
	7.4	10 ± 1	258 ± 67	0.005 ± 0.001